INTERNATIONAL JOURNAL OF INTELLIGENT CONTROL AND SYSTEMS
VOL. 14, NO. 2, JUNE 2009, 166-172

Combining Nonlinear Fractal Transformation and Neural Network Based Classifier for Cardiac Arrhythmias Recognition

[1]Chia-Hung Lin, [2]Chao-Lin Kuo, [1]Jian-Liung Chen, and [3]Wei-Der Chang

***Abstract*—**This paper proposes a method for cardiac arrhythmias recognition using fractal transformation (FT) and neural network based classifier. Iterated function system (IFS) uses the non-linear interpolation in the map and FT with fractal dimension (FD) is used to construct various fractal patterns, including supra-ventricular ectopic beat, bundle branch ectopic beat, and ventricular ectopic beat. Probabilistic neural network (PNN) is used to recognize normal heartbeat and multiple cardiac arrhythmias. The proposed classifier is tested using the MIT-BIH (Massachusetts Institute of Technology-Beth Israel Hospital) arrhythmia database. Compared with other method, the results will show the efficiency of the proposed method, and also show high accuracy for recognizing electrocardiogram (ECG) signals.

***Keywords*—**Fractal Transformation (FT), Iterated Function System (IFS), Non-linear Interpolation, Fractal Dimension (FD), Probabilistic Neural Network (PNN), Electrocardiogram (ECG).

1. Introduction

ECG signal is a recording of the cardiac-induced skin potentials at the body's surface, reveals information of atrial and ventricular electrical activity. The electrical activity of heartbeat is influenced by many physiological mechanisms. Electrocardiography is used to diagnose the variety of pathologies that affect the cardiovascular system, and serve to expose and distinguish cardiac dysfunction [1]. Cardiac arrhythmias are not fatal diseases but may require therapy to prevent further problems. Electrocardiograph (Holter recorder) is used to record the electrical activity with surface electrodes on the chest, such as devices can record large amounts of signals, but do not automatically classify abnormalities and require off-line analysis. An ECG signal consists of P-wave, QRS complexes, and T-wave. QRS complex is the information for cardiac arrhythmias classification. For developing automated detector, diagnostic methods have been applied to detect cardiac arrhythmias with time domain, frequency domain, and time-frequency domain techniques. Different electrical potentials of the heartbeat provide the information of disturbances in the normal electrical activity. In the time domain, ECG features are heartbeat interval (RR-interval), amplitude parameters (QRS, ST, P, Q, R, & S), duration parameters (PR, QRS, & QT), QRS morphology, combined parameters, and area of QRS complex, etc. [2]-[3]. For frequency-domain technique, power spectra of the QRS complex are found at 4, 8, 12, 16, and 20Hz. The spectrum has the maximum amplitude at 4Hz in ventricular tachycardia (VT), and its amplitude decreases as the frequency increases [4]. In the time-frequency technique, wavelet transform (WT) has applied to extract the features of cardiac arrhythmias by using discrete wavelet transform [5]-[6]. WT is robust to time-varying signal analysis, but it is not capable of recognition. Artificial-intelligent (AI) methods have been proposed to classify the cardiac abnormalities including artificial neural network (ANN) [4], wavelet neural networks [5]-[7], Fuzzy hybrid neural networks [8], and grey relational analysis [9].

Time-frequency domain technique has proposed to analyze the time-varying signals. However, it needs to choice wavelet shape, wavelet type, and determine the wavelet coefficients. The ANN approach is well known for its learning and recognition ability, and provides promising results in pattern recognition and diagnosis classification tasks. Traditional neural networks are limited to the problems of determining architectures of supervised learning. The local minimum problem, slow learning speed, and the weight interferences between different patterns are the major drawbacks. Considering these limitations, nonlinear interpolation fractal model and probabilistic neural network (PNN) are employed to develop a classifier. Nonlinear interpolation function transforms segment maps to the fractal features of typical cardiac arrhythmias. PNN is used to recognize normal and abnormal ECG signals.

According to the Association for the Advancement of Medical Instrumentation (AAMI) [2] recommended standard, heartbeat classes are recommended including the normal beat, supra-ventricular ectopic beat, bundle branch ectopic beat, ventricular ectopic beat, fusion beat, and unknown beat. Test data are obtained form MIT-BIH arrhythmias database. The results will show computational efficiency and accurate recognition for recognizing ECG signals.

2. Mathematical Method Description

2.1 Fractal Transformation (FT)

Iterated function system (IFS) has been proposed for signal modeling. An IFS is simple in form and capable of producing complicated functions which are fractal in nature [10]-[11]. It has been used to create images and various waveforms that resemble those found naturally. The fractal method of modeling data involves selecting interpolation points from the sampling data and creating IFS maps. These maps can be used to recreate the

Corresponding author: **Chia-Hung Lin**
[1]Chia-Hung Lin and Jian-Liung Chen are with the Department of Electrical Engineering, Kao-Yuan University, Lu-Chu Hsiang, Kaohsiung county 821, Taiwan (E-mail: eechl53@educities.edu.tw).
[2]Chao-Lin Kuo is with the Department of Electrical Engineering, Far-East University, Hsin-Shih Township, Tainan County, 744, Taiwan (E-mail: clkuo@cc.feu.edu.tw).
[3]Wei-Der Chang is with the Department of Computer and Communication, Shu-Te University, Yen-Chau, Kaohsiung County 824, Taiwan (E-mail: wdchang@mail.stu.edu.tw).

original data. An IFS is a finite set of contraction mappings for interpreting the data to be modeled as a graph. In modeling the graph of a function or data sequence $x[n]$, n=1, 2, 3, …, N, the P interpolation maps, w_j, j=1, 2, 3, …, P, can be presented as [10]-[11]

$$w_j\left(\begin{bmatrix} n \\ x[n] \end{bmatrix}\right) = \begin{bmatrix} a_j & b_j \\ c_j & d_j \end{bmatrix}\begin{bmatrix} n \\ x[n] \end{bmatrix} + \begin{bmatrix} e_j \\ f_j \end{bmatrix} \tag{1}$$

$$\begin{cases} w_j(n) = a_j n + b_j x[n] + e_j \\ w_{jx}(x[n]) = c_j n + d_j x[n] + f_j \end{cases} \tag{2}$$

Equation (1) can be separated into two equations $w_j(n)$ and $w_{jx}(x[n])$. The b_j term is set to be zero, confirming that the resulting attractor is single-valued. The interpolation points fix the a_j and e_j terms as [12]

$$a_j = \frac{M_{j2} - M_{j1}}{N-1}, \quad e_j = M_{j1} \tag{3}$$

For each j, the w_j maps the data sequence $x[n]$ onto the subsequences with interpolation points M_j in the interval $[M_{j1}, M_{j2}]$, and the maps can be constructed adjacently. The method has two stages: first to determine the interpolation points, and second to determine the best map parameters. The remaining map parameters c_j, d_j, and f_j can be solved by minimizing the sum of squared errors between the transformed data and the original data in the range of the jth map, and can be justified by the Collage Theorem [13]:

$$e_j = \sum_{i=M_{j1}}^{M_{j2}} (w_{jx}(x[n]) - x[i])^2 \tag{4}$$

where $n = \text{int}[(\frac{i - M_{j1}}{M_{j2} - M_{j1}})(N-1)]$, and $M_j = M_{j2} - M_{j1} + 1$.

IFS is implemented with similarity maps, the resulting data is "self-similarity". To improve the self-similarity constraint, nonlinear interpolation is used in the maps and makes the model flexibility. The remaining map parameters c_j, d_j, f_j , g_j and h_j can be solved by

$$\sum_{i=1}^{M_j} [S_i \cdot S_i^T] \begin{bmatrix} c_j \\ d_j \\ f_j \\ g_j \\ h_j \end{bmatrix} = \sum_{i=1}^{M_j} S_i \cdot x[i] \tag{5}$$

$$S_i = \left[n' \quad x[i] \quad 1 \quad \sin(\frac{\pi n'}{D}) \quad \sin(\frac{2\pi n'}{D}) \right]^T, \quad n' = (\frac{D-1}{M_j - 1})i$$

For j maps, j=1, 2, 3, …, P, data sequence $x[i]$, i=1, 2, 3, .., M_j, onto each fractal map can be modified as

$$\varphi_{ji} = c_j n' + d_j x[i] + f_j + g_j \sin(\frac{\pi n'}{D}) + h_j \sin(\frac{2\pi n'}{D}) \tag{6}$$

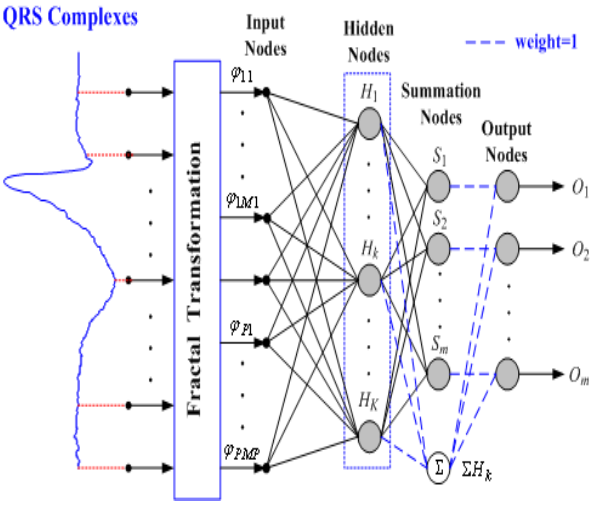

Figure 1. Architecture of the probabilistic neural network

where D is fractal dimension (FD) and has a dimension between 1 and 2. Fractal dimension will changes ECG signals to fractal features at different scales. Input sequences $x[i]$ are the sample data from the QRS complexes. Fractal maps can be constructed as

$$\Phi(\varphi_{ji}) = \bigcup_{j=1}^{P} \varphi_{ji}, \quad i=1, 2, 3, \ldots, M_j \tag{7}$$

Equation (7) is used to extract the features from the ECG signals, and equation (8) is applied to construct the fractal features of normal beat and abnormal beat, as

$$\Phi(k) = [\varphi_{11}(k), \ldots, \varphi_{1M1}(k), \ldots, \varphi_{j1}(k), \ldots, \varphi_{jMj}(k), \ldots, \varphi_{P1}(k), \ldots, \varphi_{PMP}(k)], \quad k=1, 2, 3, \ldots, K \tag{8}$$

where K is the number of training data for neural network. These cardiac features include the normal beat (•), atrial premature beat (**A**), premature ventricular contraction (**V**), right bundle branch block beat (**R**), left bundle branch block beat (**L**), paced beat (**P**), and fusion of paced and normal beat (**F**).

2.2 Probabilistic Neural Network (PNN)

Probabilistic neural network (PNN) consists of input, hidden, summation, and output layer is shown in Figure 1. The input vector $\Phi = [\varphi_{11}, \ldots, \varphi_{1M1}, \ldots, \varphi_{j1}, \ldots, \varphi_{jMj}, \ldots, \varphi_{P1}, \ldots, \varphi_{PMP}]$ is connected to the PNN, and inputs are the fractal features from the QRS complexes. The number of hidden nodes H_k (k=1, 2, 3, …, K) is equal to the number of training data, while the number of summation nodes S_t and output nodes O_t (t=1, 2, 3, …, m) equals to the classified types. The weights w_{ki}^{IH} (connecting the hidden nodes and the input nodes) and w_{tk}^{HS} (connecting the summation nodes and the hidden nodes) are determined by K input-output training pairs. The final output of node O_t is [14]

$$H_k = \exp[-\sum_{k=1}^{K} \frac{(\varphi_{ji} - w_{ki}^{IH})^2}{2\sigma_k^2}] \tag{9}$$

$$O_t = \frac{\sum_{k=1}^{K} w_{tk}^{HS} H_k}{\sum_{k=1}^{K} H_k}, \quad t=1, 2, 3, \ldots, m \tag{10}$$

The optimal σ_k is intended to minimize the predicted squared error function $e_t(\varphi, T) = [T_t - O_t(\varphi)]^2$, where T_t is the desired output for input vector Φ. The optimization method is used to adjust parameter σ_k with iteration process [14]-[15], as in equation (11)

$$\sigma_k(Itr+1) = \sigma_k(Itr) + \eta \frac{\partial e_t(\varphi, T)}{\partial \sigma_k} \tag{11}$$

where η is the learning rate, and *Itr* is the iteration number. The algorithm of the PNN contains two stages: "*Learning Stage*" and "*Recalling Stage*", as detailed below.

2.2.1. Learning Stage

Step 1)For each training data $\Phi(k)= [\varphi_{11}(k), \ldots, \varphi_{1M1}(k), \ldots, \varphi_{j1}(k), \ldots, \varphi_{jMj}(k), \ldots, \varphi_{P1}(k), \ldots, \varphi_{PMP}(k)]$, k=1, 2, 3, …, K, i=1, 2, 3, …, M_j, and j=1, 2, 3, …, P, create weights w_{ki}^{IH} between input node and hidden node by

$$w_{ki}^{IH} = \Phi(k) \tag{12}$$

Step 2)Create weights w_{tk}^{HS} between hidden node H_k and summation node S_t by

$$w_{tk}^{HS} = \begin{cases} 1 \\ 0 \end{cases} \quad (t=1, 2, 3, \ldots, m) \tag{13}$$

where the values of w_{tk}^{HS} are the predicted outputs associated with each stored pattern w_{ki}^{IH}. Connection weights from hidden nodes H_k to summation node Σ are set 1.

2.2.2. Recalling Stage

Step 1)Get network weights w_{ki}^{IH} and w_{tk}^{HS}.
Step 2)Apply test vector $X=[x_{11}, \ldots, x_{1M1}, \ldots, x_{j1}, \ldots, x_{jMj}, \ldots, x_{P1}, \ldots, x_{PMP}]$ to the fractal transformation function. Compute the fractal features Φ by

$$\varphi_{ji} = c_j n' + d_j x_{ji} + f_j + g_j \sin(\frac{\pi n'}{D}) + h_j \sin(\frac{2\pi n'}{D}) \tag{14}$$

$$\Phi(\varphi_{ji}) = \bigcup_{j=1}^{P} \varphi_{ji}, \quad i=1, 2, 3, \ldots, M_j \tag{15}$$

Step 3)Compute the output of hidden node H_k, k=1,2, 3, …, K, by Gaussian activation function

$$H_k = \exp[-\sum_{k=1}^{K} \frac{(\varphi_{ji} - w_{ki}^{IH})^2}{2\sigma^2}] \tag{16}$$

where $\sigma_1=\sigma_2=\ldots=\sigma_k=\ldots=\sigma_K=\sigma$. the optimal value can be obtained by using optimization method.
Step 4)Compute the outputs of node O_t by using the equation (10).

3. Features Creation

In this study, the datasets of QRS complexes are taken from the MIT-BIH arrhythmias database (from Record 100 to Record 233) [16]. The subjects are 25 men aged 32 to 89 years, and 22 women aged 23 to 89 years. The records include complex ventricular, junctional, supra-ventricular arrhythmias, and conduction abnormalities. According to the AAMI recommended standard [2], the cardiac disorders can be classified into seven categories. In these records, the upper signal is a modified limb lead II (ML II), and the lower signal is a modified lead V1 (Occasionally V2 or V5, and in one instance V4). ECG has come to Excel workspace at visually interpreting the form of the ECG wave pattern and has become adept at different diagnoses. An ECG signal represents the changes in electrical potential during the heartbeat as recorded with non-invasive electrodes on the limbs and chest; a typical ECG signal consists of the P-wave, QRS complex and T-wave. The morphology of ECG signal varies with rhythm origin and conduction path. When the activation pulse originates in the ventricle and does not travel through the normal conduction path, the QRS complex becomes distorted morphological features. The QRS complex is some distinct information in heart-rate monitoring and cardiac diseases diagnosis.

In the preprocessing step, R-wave peak are detected by the peak detection algorithm or Tompkins algorithm [4, 17]. R-wave peak detection begins by scanning for local maxima in the absolute value of ECG data. For certain window duration, the searching continues to look for a larger value. If this search finishes without finding a larger maximum, the current maximum is assigned as the R-wave peak [4]. Centered on the detected R-wave peak, the QRS complex portion is extracted by applying a window of 280ms, and P-wave and T-wave are excluded by this window duration. Based on 180 sampling rate, 50 samples can be acquired around the R-wave peak (Sampling point N=50, 25 points before and 25 points after). After sampling and analog-to-digital conversion individual QRS complexes are extracted in the time-domain. Each sample is preprocessed by removing the mean value to eliminate the offset effect and dividing with the standard deviation. Overall QRS complexes could be selected from patient numbers 100, 103, 107, 109, 111, 118 119, 124, 200, 202, 207, 209, 212, 213, 214, 217, 221, 231, 232, and 233. From subject records, 43 QRS complexes are picked up and classified into seven types. Symptomatic patterns are produced by the nonlinear interpolation function and linear interpolation function. Centered on the R-wave peak, the QRS complex of normal beat (Patient Number: 200) can be divided into two segments, segment number j=1, 2, and

Table 1. The remaining map parameters of linear and nonlinear interpolation function

Model	Fractal Map	Remaining Map Parameter				
		c_j	d_j	f_j	g_j	h_j
Nonlinear Interpolation	φ_1	0.9005	0.8253	0.4846	0.4358	-0.1810
	φ_2	-0.5080	0.8810	-0.1110	0.5657	-0.1246
Linear Interpolation	φ_1	-0.0093	0.0091	-0.0541	—	—
	φ_2	0.4397	0.6946	0.5213	—	—

Note: Linear Interpolation Function: $\varphi_j = c_j i + d_j x[i] + f_j$, j=1, 2.

$$\sum_{i=1}^{M_j} [S_i \cdot S_i^T] \begin{bmatrix} c_j \\ d_j \\ f_j \end{bmatrix} = \sum_{i=1}^{M_j} S_i \cdot x[i], \quad S_i = [i \quad x[i] \quad 1]^T .$$

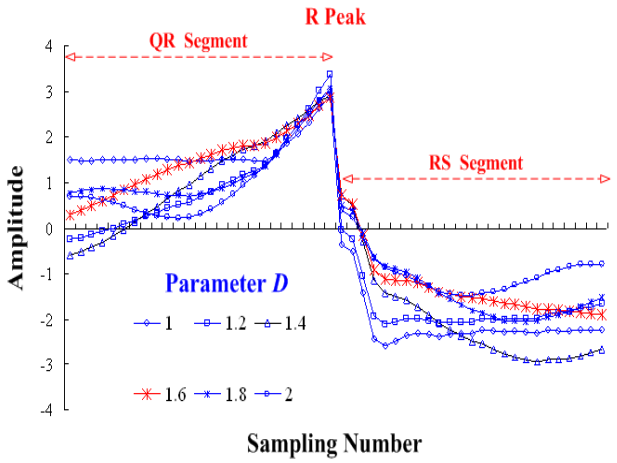

Figure 2. Fractal features extraction using nonlinear interpolation function with various fractal dimensions.

sampling points M_j=25 (N=M_1+M_2=50). The remaining map parameters can be solved by equation (5). Fractional patterns are constructed with equations (6) and (7). By using fractal dimension between 1.0 and 2.0, fractional patterns with various fractal dimensions are shown in Figure 2. Nonlinear interpolation function with fractal dimension D=1.6 is chosen in this study, and the related remaining map parameters are shown in Table 1. With the same samples, the parameters of linear interpolation are solved and also shown in Table 1. Fractal symptomatic patterns with nonlinear and linear interpolation functions are shown in Figure 3. Overall values of fractal patterns in Figure 3 are outside the interval [0 12] and [-4 4], respectively, where the horizontal axis is the sample number, and the vertical axis is the fractal feature. For 43 QRS complexes, fractal patterns are produced by the linear interpolation function. It is not obviously to distinguish the symptomatic types from the linear interpolation patterns. ECG signals are irregular in their inflections and have different shapes for different patients. So we choose the nonlinear FT to recreate the symptomatic patterns.

These features have various morphological could be used to discriminate the arrhythmic types including normal beat (•), **V**, **A**, **L**, **R**, **P**, and **F**. With the data self-similarity, amount of data set can be reduced for the same type (decreases from 43 to 25). The numbers of QRS complexes from the same class are 1-, 6-, 2-, 6-, 4-, 4-, and 2-set data respectively. According to the various

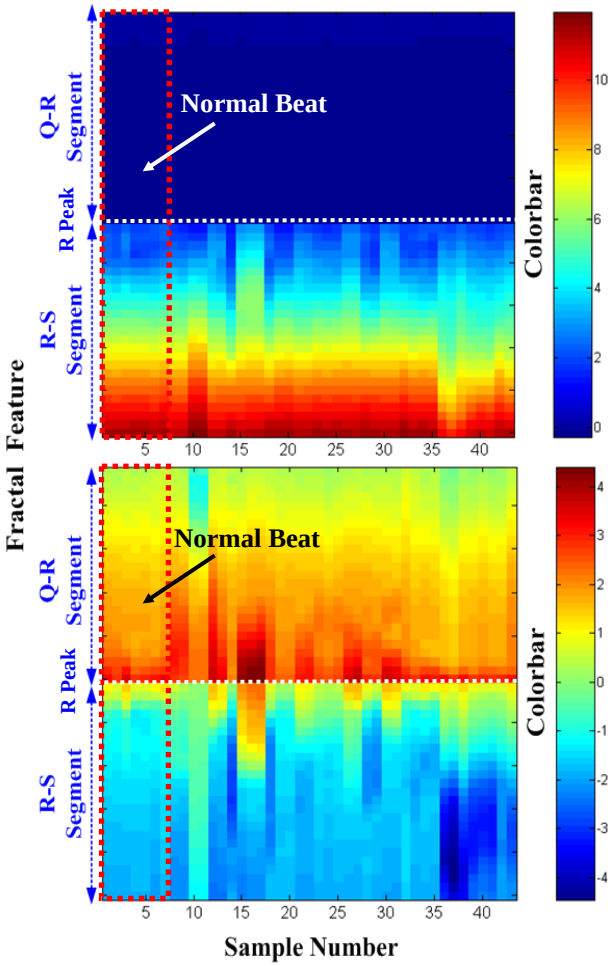

Note:(1) No. 1~7: •; (2) No. 8~18: V; (3) No. 19~20: A; (4) No. 21~28: L; (5) No. 29~36: R; (6) No. 37~41: P; (7) No. 42~43: F.

Figure 3. Various fractal patterns with FT. (a) QRS complex extraction using linear interpolation function; (b) QRS complex extraction using nonlinear interpolation function with fractal dimension D=1.6.

symptomatic patterns, we can systematically create training data $\Phi(k)$ with equations (6), (7), and (8). The number of training data is equal to 25-set data (K=25). For the classification of seven classes, the associated classes could be expressed as weighting factors. The weights w_{tk}^{HS}, k=1, 2, 3, …, 25, t=1, 2, 3, …, 7, are encoded as binary values by equation (12) with signal "1" for belonging to *Class m* and the rest of the weights are zero. The PNN contains 50 input nodes, 25 hidden nodes, 8 summation nodes, and 7 output nodes. The number of input nodes is equal to the number of the sampling points, the number of hidden nodes is equal to the number of training data, and each output represents one normal beat and six types of arrhythmias as defining output vector O=[O_{Nor}, O_V, O_A, O_L, O_R, O_P, O_F]. The selection sort is applied to find the maximum value that indicates the arrhythmic type. The output values are between 0 and 1, where a value close to 1 means "*Normal*", and close to 0 means "*Abnormal*".

4. Experiment Results

The proposed detection method was developed on a

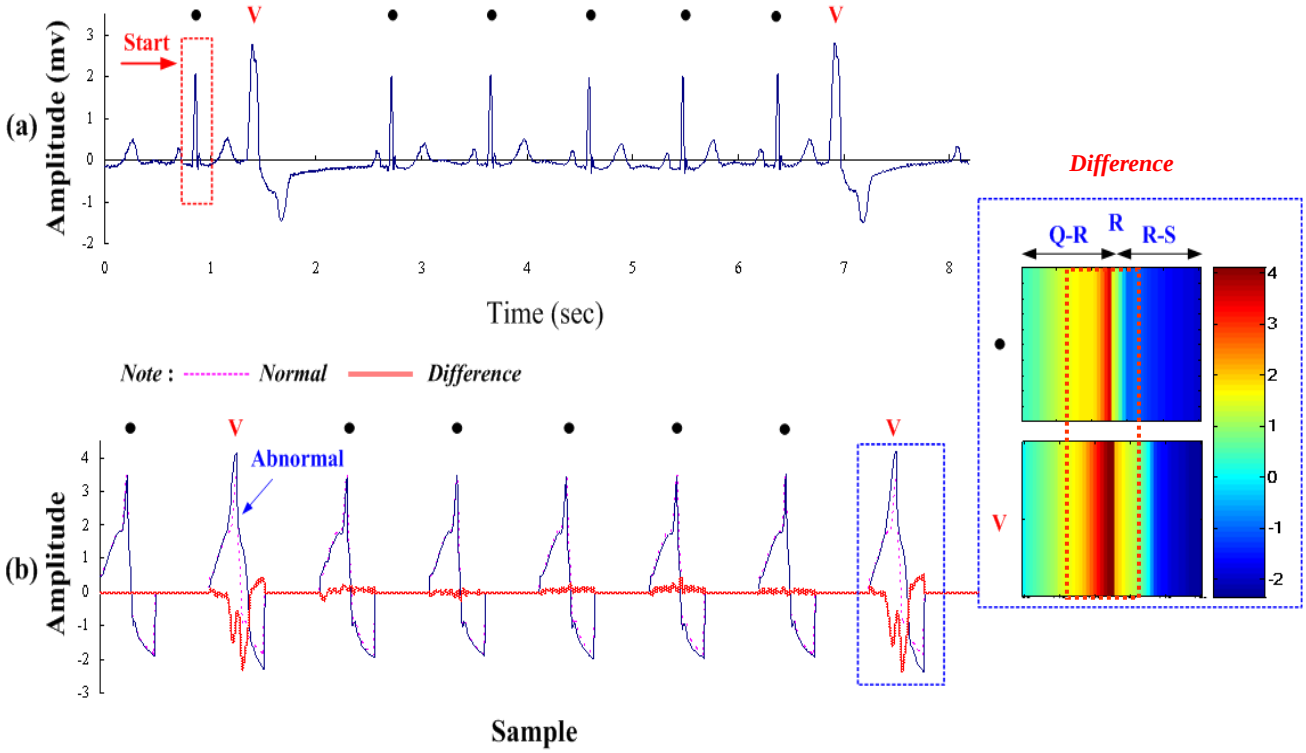

Figure 5. (a) ECG signals of normal beat and V (Record 119, ML II Signal) (b) Symptomatic patterns of normal (•) beat and **V**

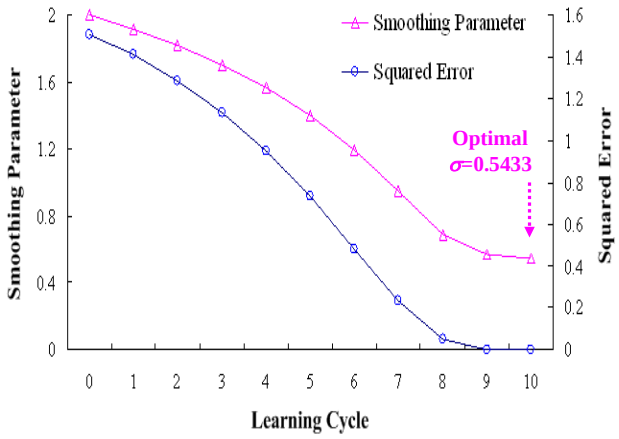

Figure 4. Squared errors and smoothing parameters versus learning cycles

PC Pentium-IV 3.0GHz with 480MB RAM and Matlab software, based on the MIT-BIH arrhythmias database including patient numbers 100, 103, 107, 109, 111, 118 119, 124, 200, 202, 207, 209, 212, 213, 214, 217, 221, 231, 232, and 233. Overall diagnostic procedures for ECG recognition divided into three stages: (1) signal preprocessing; (2) fractal trandformation; (3) heart beat recognition with PNN. We have 25-set training data for PNN with the seven classes. The gradient method is used to adjust smoothing parameter σ with iteration process [14]. For the convergent condition (*Squared Error*$\leq 10^{-3}$), PNN converges to the nearest local minimum for less than 10 learning cycles in a shorter processing time. It takes 0.2970 seconds to classify the 25 training data into seven categories. The optimal parameter σ=0.5433 can minimize the classification error. Figure 4 shows the squared errors and smoothing parameters versus learning cycles, respectively. The performance of the proposed method was tested with diagnostic accuracy for unrecorded data, as detailed below.

Table 2. The results of multiple cardiac arrhythmias

Record		Number of Arrhythmias							CPU Time (sec)	Accuracy (%)
		•	V	A	L	R	P	F		
107	Actual	0	0	0	0	0	100	0	—	—
	Test1	0	3	0	0	0	96	1	1.097	96
	Test2	0	0	0	0	0	96	4	1.105	96
119	Actual	75	25	0	0	0	0	0	—	—
	Test1	75	25	0	0	0	0	0	1.100	100
	Test2	75	25	0	0	0	0	0	1.110	100
200	Actual	62	38	0	0	0	0	0	—	—
	Test1	61	32	0	1	6	0	0	1.134	93
	Test2	60	32	0	3	5	0	0	1.191	92
212	Actual	5	0	0	0	95	0	0	—	—
	Test1	5	0	0	0	95	0	0	1.169	100
	Test2	5	0	0	0	95	0	0	1.125	100
214	Actual	0	5	0	95	0	0	0	—	—
	Test1	1	4	1	92	2	0	0	1.187	96
	Test2	1	5	3	91	0	0	0	1.150	96
217	Actual	0	3	0	0	0	94	3	—	—
	Test1	1	3	0	0	0	91	5	1.119	97
	Test2	1	3	0	0	0	90	6	1.197	96

Note: (1) Accuracy(%)=(N_r/N_t)×100%, the overall accuracy is the fraction of the total heartbeats correctly classified. (2) N_r: the number of correctly discriminated beats; N_t: total number of heartbeats.

4.1 Single Cardiac Arrhythmia

The features are used for extraction from QRS complexes within the movable window with each shift in time. The content of each window is applied to the proposed diagnostic procedure. Figure 5 shows the ECG

signals of normal heartbeat (•) and premature ventricular contraction (**V**) in the time domain and the symptomatic patterns, respectively. After feature extraction with nonlinear interpolation function, the same types always have similar symptomatic patterns. When a QRS complex has different pathological shape in the QR-segment or RS-segment due to rhythm origin and conduction abnormalities, the differences ($Difference(M_j) = \Phi_{Nor}(M_j) - \Phi_V(M_j)$, j=1, 2) will obviously reveal the rise or dip characteristics as shown in Figure 5. For example, using 100 heartbeats (about 1.5min long) of the patient numbers 119 and 200 containing normal beats and **V**-beats, Test 1 show that the overall accuracies are 100% and 93% as shown in Table 2, respectively. For patient number 200, the processes recognized 38 **V**-beats with 6 failures, and the expect sensitivities as the fraction of the class **V** correctly classified are respectively 100% and 80%, and the specificity for normal heartbeats is 100%. The results confirm that the major class is premature ventricular contraction.

Ventricular ectopic beats are multiform waveforms, and are different for different patients and even for the same patient or for the same type. Patient number 200 is a special case, including ventricular bigeminy (**(B**), ventricular, ventricular tachycardia (**(VT**), and are occasional bursts of high-frequency noise in the ECG signals [16]. These signals may be disturbed by noise such as power line interference (50Hz/60Hz interference). The proposed method does not promise results with 100% accuracy due to some **(B**-beats are similar to **R**-beats and severe noise. Test 2 shows the results of ECG signals involving noisy interference as shown in Table 2. In clinical diagnosis, positive predictivity (PP) of more than 80% is obtained to quantify the performance of proposed method without or with a noisy background. The inclusion of the irregular beats slightly affects the efficiency of the proposed method. In the real world, the notch filter can be used to remove unwanted frequency interference and artifact noise. This can support that the proposed method can work under a noisy environment for the diagnosis.

4.2 Multiple Cardiac Arrhythmias

Clinical diagnostic subjects have multiple cardiac arrhythmias such as supraventricular ectopic beat, ventricular ectopic beat, bundle branch ectopic beat, fusion, and paced beats. For example, patient numbers 214 and 217 have premature ventricular contraction (**V**), left bundle branch block beat (**L**), paced beat (**P**), and fusion of paced and normal beat (**F**). As seen in Table 2, the results of Test 1 confirm that the major cardiac arrhythmias are class **L** and class **P**. The processes recognized 95 **L**-beats with three failures, and 94 **P**-beats with four failures. The sensitivity (SE) is defined as $SE=TP/(TP+FN)$, TP defines beats that have been correctly assigned to a certain class. FN occurs when beats should have been assigned to that class but are missed and assigned to another class. The SEs for major ectopic beats are 96.93% and 96.90%, and the overall accuracies are 96% and 97%, respectively. Test 2 shows the results of multiple cardiac arrhythmias involving noisy interference as shown in Table 2. The proposed method can also recognize multiple cardiac arrhythmias with good accuracy.

Table 3. Comparison of proposed method with WMLNN

Method	Network Topology	Training Patterns	Learning Rate η	Learning Cycles	Average CPU Time (s)
Proposed Method	50-25-8-7	25	0.1~03	≤ 10	0.2970
WMLNN	(1) 50-50-29-7 (2) 50-50-57-7	43	0.2~0.8	< 5000	< 200

Note: (1) $N_H=(N_I+N_O)/2$; (2) $N_H=(N_I+N_O)$. N_H: the number of hidden node; N_I: the number of input node; N_O: the number of output node [7].

4.3 Compare the proposed method with WMLNN

In order to show the effectiveness of the proposed method, we have also applied the WMLNN composed of 50 wavelet nodes in the wavelet layer and a multi-layer neural network (WMLNN). For the second subnetwork, a WMLNN is used for training with the back-propagation learning algorithm. Only one hidden layer is used, and the number of hidden nodes is determined by the experience formulas [7] as shown in Table 3. The WMLNN has some limitations including very slow learning process, need iteration for determining weights and learning rates, and need to determine the network architecture such as the number of hidden layers and hidden nodes. As the number of training data increases, training process and classification efficiency become a main problem. The wavelet transform (WT) could affect reconstructed signal quality, thus the wavelet coefficients need to be chosen. Significant features are suited to classify different patterns at specific dilation and translation parameter, where dilation parameter=3 and 50 translation parameters for extracting features under low frequency analysis, and these features are reconstructed by 50 wavelet nodes (Morlet Wavelet) to form the symptomatic patterns [7]. Owing to the data self-similarity using the FTs, the requirement of training data (from 43-set to 25-set training data), data storage, and network topology can be reduced. The non-linear interpolation function needs less parameter assignment for constructing FTs with 5 remaining map parameters for the Q-R segment and R-S segment, respectively. The outcomes of the proposed method are better than other hybrid method as shown in Table 3.

5. Conclusion

A classifier using fractal transformation (FT) and probabilistic neural network (PNN) has been developed to recognize the states of cardiac physiologic function. Iterated function system (IFS) is proposed for modeling the FT function. It consists of sinusoidal terms to the affine maps, and its form with non-integer fractal dimension (FD) acts to extract the features from QRS complexes in the time domain, including both “Q-R segment” and “R-S segment”. FT functions make fractal patterns more distinguishing between normal and ill subjects. Then PNN uses these patterns to recognize the cardiac arrhythmias with and without a noisy background.

The PNN can automatically construct the network and adjust the smoothing parameters of hidden nodes using optimization method. It has the ability to expand/reduce network structure with add-in/delete-off training patterns. With this flexible model, new patterns can be further added to the current database without the trial-and-error procedure. Compared with other method, the proposed method shows higher accuracy, faster processing time, and less data and parameters required.

6. Acknowledgment

This work is supported in part by the National Science Council of Taiwan under contract number: NSC97-2221-E-244-001 **(August 1 2008~July 31 2009)**.

7. Reference

[1] Metin Akay, "Nonlinear Biomedical Signal Processing-Dynamic Analysis and Modeling Volume II, "The Institute of Electrical and Electronics Engineers, Inc. New York, 2001.
[2] Philip de Chazal, Maraia O' Dwyer, and Richard B. Reilly, "Automatic Classification of Heartbeats Using ECG Morphology and Heartbeat Interval Features, "IEEE Transactions on Biomedical Engineering, Vol. 51, No. 7, July 2004, pp. 1196-1206.
[3] Giovanni Bortolan, Christian Brohet, and Sergio Fusaro, "Possibilities of Using Neural Networks for ECG Classification, " Journal of Electrocardiology, Vol. 29 (Supplement), pp. 10-16.
[4] Kei-ichiro Minami, Hiroshi Nakajima, and Takesshi Toyoshima, "Real-Time Discrimination of Ventricular Tachyarrhythmia with Fourier-Transform Neural network, "IEEE Transactions on Biomedical Engineering, Vol. 46, No. 2, February 1999, pp. 179-185.
[5] Shuren Qin, Zhong Ji, and Hongjun Zhu, "The ECG Recording Analysis Instrumentation Based on Virtual Instrument Technology and Continuous Wavelet Transform, "Proceedings of the 25th Annual International Conference of the IEEE EMBS Cancun, Mexico, September 17-21, 2003, pp. 3176-3179.
[6] Hartmut Dickhaus and Hartmut Heinrich, "Classifying Biosignals with Wavelet Networks-A Method for Noninvasive Diagnosis, " IEEE Engineering in Medicine and Biology, September/October 1996, pp. 103-111.
[7] Chia-Hung Lin, Yi-Chun Du, and Tainsong Chen, "Adaptive Wavelet Network for Multiple Cardiac Arrhythmias Recognition , "Expert Systems with Applications, Vol. 34, No. 4, May 2008, pp. 2601-2611.
[8] Yang Wang, Yi-Sheng Zhu, Nitish V. Thakor, and Yu-Hong Xu, "A Short-Time Multifractal Approach for Arrhythmias Detection Based on Fuzzy Neural Network, "IEEE Transactions on Biomedical Engineering, Vol. 48, No. 9, September 2001, pp. 989-995.
[9] Chia-Hung Lin, "Classification Enhancible Grey Relational Analysis for Cardiac Arrhythmias Discrimination, "Medical & Biological Engineering & Computing, Vol. 44, No. 4, April 2006, pp. 311-320.
[10] D. S. Mazel and M. H. Hayes, "Using Iterated Function Systems to Model Discrete Sequences, "IEEE Transaction on Signal Processing, Vol. 40, No. 7, July 1992, pp. 1724-1734.
[11] Greg Vines and Monson H. Hayes, III, "Nonlinear Address Maps in a One-Dimensional fractal Model, "IEEE Transactions on Signal Processing, Vol. 41, No. 4, April 1993, pp. 1721-1724.
[12] Michael Barnsley, "Fractal Functions and Interpolation, " Constructive Approximation, 2:303-329, 1986.
[13] Michael Barnsley, Fractals Everywhere, Academic Press, Inc., New York, N. Y., 1988.
[14] Chia-Hung Lin and Chia-Hao Wang, "Adaptive Wavelet Networks for Power Quality Detection and Discrimination in a Power System, "IEEE Transactions on Power Delivery, Vol. 21, No. 3, July 2006, pp. 1106- 1113.
[15] Teo Lian Seng, Marzuki Khalid, and Rubiyah Tusof, "Adaptive GRNN for the Modeling of Dynamic Plants, "Proc. of the 2002 IEEE International Symposium on Intelligent Control Vancouver, Canada, October 27-30, 2002, pp. 217-222.
[16] Goldberger AL, Amaral LAN, Glass L, Hausdorff JM, Ivanov PCh, Mark RG, Mietus JE, Moody GB, Peng CK, Stanley HE. PhysioBank, Physio Toolkit, and PhysioNet: Components of a New Research Resource for Complex Physiologic signals. Circulation 101(23):e215-e220[Circulation electronic Pages; http://circ/cgi/content/full/101/23/e215]; 2000 (June 13).
[17] Pan, J and W. J. Tompkins, "A Real-time QRS Detection Algorithm, "IEEE Transactions on Biomedical Engineering, Vol. 32, No. 3, 1985, pp. 230-236.

8. Biographies

Chia-Hung Lin was born in 1974. He received the B.S. degree in electrical engineering from the Tatung Institute of Technology, Taipei, Taiwan, in 1998, the M.S. degree in electrical engineering from the National Sun Yat-Sen University, Kaohsiung, Taiwan, in 2000, and the Ph.D. degree in electrical engineering from National Sun Yat-Sen University in 2004. Currently, he is a teacher of department of electrical engineering, Kao-Yuan University, Lu-Chu Hsiang, Kaohsiung, Taiwan, where has been since 2004.

His research interests include fault diagnosis in power system, neural network computing, and harmonic analysis. Currently, his area of interest is biomedical signal processing and pattern recognition.

Chao-Lin Kuo received the B.S. degree from the Department of Automatic Control Engineering, Feng Chia University, Taichung, Taiwan, Republic of China, in 1998, and M.S. degree from the Institute of Biomedical Engineering, National Cheng Kung University, Tainan, Taiwan, Republic of China, in 2000. In 2006, he received his Ph.D. degree in Department of Electrical Engineering, National Cheng Kung University, Tainan, Taiwan, Republic of China. He has been with the Department of Electrical Engineering, Far East University since 2004, and is currently an assistant Professor.

His current research interests include intelligent control systems, fuzzy systems, and embedded systems and its applications.

Jian Liung Chen received the Ph.D. degree in electrical engineering from National Sun Yat-Sen University in 2003. Currently, he is the assistant professor of department of electrical engineering, Kao-Yuan University, Lu-Chu Hsiang, Kaohsiung, Taiwan, where has been since 2005.

His research interests include LMI approach in control, robust control, descriptor system theory, digital signal processing, and pattern recognition.

Wei-Der Chang was born in Kaohsiung, Taiwan in 1970. He received his Ph.D. degree in the electrical engineering from National Sun Yat-Sen University, Kaohsiung, Taiwan, in 2002. He is now an Associate Professor at the Department of Computer and Communication, Shu-Te University, Kaohsiung, Taiwan, where has been since 2002.

His research interests include the digital signal processing, digital filter designs, evolutionary computations, chaotic secure communication, and control engineering.